The influence of applied stress on precipitate shape and stability

M. B. Berkenpas, William C. Johnson, and D. E. Laughlin
Department of Metallurgical Engineering and Materials Science, Carnegie–Mellon University, Pittsburgh, Pennsylvania 15213

(Received 19 May 1986; accepted 5 September 1986)

Shape transitions and orientation alignment of elastically misfitting precipitates in the presence of an external stress field have been predicted using bifurcation and group theory and by performing actual energy calculations for elliptical cylinders under plane strain conditions. Under the assumption of system isotropy, the applied field acts to break or perturb the bifurcation. Both first- and second-order size-induced shape transitions are observed for elastically soft precipitates. Stress-induced shape transitions are shown to be either first-order or continuous for elastically soft precipitates. Only continuous stress-induced shape transitions are observed for hard precipitates.

I. INTRODUCTION

The equilibrium shape of an isolated precipitate in a two-phase alloy is determined by minimizing the sum of the elastic strain energy and the interfacial energy. The shape that minimizes the elastic strain energy is not necessarily equivalent to the one that minimizes the interfacial energy. Because the elastic strain energy scales with the volume of the precipitate, V, and the interfacial energy scales as $V^{2/3}$, it is not surprising that in a number of alloy systems precipitate shape transitions are observed as a function of precipitate size.[1]

Our understanding of precipitate shape transitions can be greatly facilitated by using the properties of bifurcation theory. Bifurcation theory is a study of the branching of solutions of nonlinear equations.[2,3] The singularity in the behavior of the precipitate shape transition versus size can be compared to well-known properties of bifurcation theory. The manner in which the precipitate shape transition is altered (broken) in an external field can also be likened to the manner in which bifurcations are perturbed (broken) by imperfections. Furthermore, the generic nature of the analysis avoids the necessity of numerous system-specific energy calculations that may often obfuscate the physics of the transition. However, effective use of bifurcation theory is predicted upon a complete understanding of the symmetry of the crystals, the external influences, and the parameters that describe the precipitate shape.

Recently, Johnson and Cahn[4] used the properties of bifurcations and symmetry predictions to show how the self-energy extremizing shapes of a precipitate should change with precipitate size. Size-induced shape transitions are predicted to occur as a function of precipitate size when the precipitates are elastically softer than the matrix under the assumption of system isotropy and in the absence of an externally imposed field. For a two-dimensional system under plane strain conditions, these transitions occur primarily in a continuous fashion analogous to a second- or higher-order phase transition (supercritical bifurcation). For a three-dimensional system, the shape transition is discontinuous (transcritical bifurcation) and is analogous to a first-order phase transition. The size-induced shape transition is predicted to occur at a distinct volume or cross-sectional area, A_c, determined by the system material parameters, and is a result of the increasing importance of minimizing the elastic strain energy at larger precipitate sizes.

The equilibrium precipitate shape can change when subjected to directional external influences such as a mechanical stress, an electric field, or a magnetic field. Physically, the external influence (stress) alters the energy of the system, thereby affecting any size-induced shape transitions predicted or observed in the absence of the external influence. Many instances of precipitate shape changes resulting from an external influence have been observed experimentally.[5–10] Although precipitate shape changes are known to occur as a result of minimizing the system energy, simple relationships between material parameters are need that quantitatively describe the changes.

An analysis of the symmetry of the shape of an individual precipitate, assuming some orientation relationship of the precipitate with the matrix, can be determined from group theory principles. Kalonji and Cahn[11] used the point group intersection of the matrix and precipitate to find the form or symmetry of the precipitate that would be expected to extremize the total energy. This means that group theory can predict energy extremizing shape symmetries and the orientation in which those shapes may occur. However, they noted that group theory alone cannot predict whether the extremizing solutions are minima, maxima, or saddle points. The actual energy minimizing shape can only be determined from energy calculations. Knowledge of the extremizing orientations offers insight into the specific energy calculations that need to be made.

A further complication arises in that coherency

 0003-6951/86/050635-11$01.75

strains are known to break or lower the symmetry of the precipitate shape.[4] This means that the precipitate shapes of lowest energy are not always those predicted by symmetry dictated extrema. However, this apparent loss in symmetry is recovered when the orientations (variants) of the precipitate are taken into account.[11–13]

In this paper we examine the influence of an applied stress field on the equilibrium precipitate shape. We treat the applied stress as a perturbation of the unstressed case and examine the ways in which the perturbation can break the bifurcations observed in the absence of an applied field. Last, a discussion of orientation effects or precipitate alignment with respect to the external field will be presented.

In order to emphasize the methods of stability characterization, this work will concentrate on a plane strain situation where the precipitate has the shape of an infinite right cylinder. The intent is to determine those precipitate shapes that extremize the total system energy as a function of precipitate volume (cross-sectional area) when the precipitate and matrix are subjected to a uniaxial load applied in the two extremizing orientations predicted by the group theory.

II. MODEL

The model consists of a single isotropic precipitate, with shear modulus μ^* and Poisson's ratio ν^*, embedded coherently in a uniform infinite matrix, with elastic constants μ and ν. The precipitate shape is constrained to be an infinite cylinder (Fig. 1) and the interfacial energy density σ is independent of crystallographic orientation. The precipitate possesses a planar dilatational misfit with respect to the matrix, the dilatation being perpendicular to the cylinder axis. A uniform uniaxial stress may exist perpendicular to the cylinder axis, resulting in the system always being in a state of plane strain.

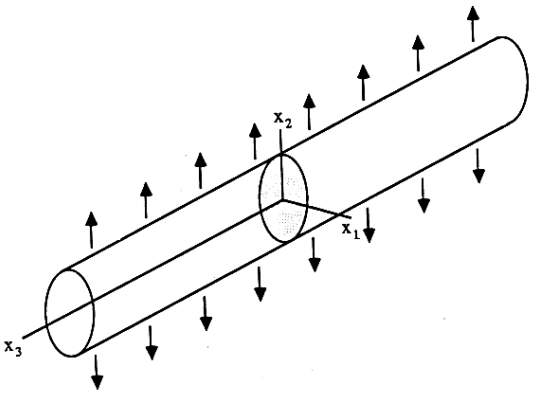

FIG. 1. Schematic depiction of the two-phase system. The semiaxes of the elliptical cross section, a and b, lie along the x_1 and x_2 axes, respectively. The applied stress, compressive or tensile, is applied along the x_2 direction. The infinite direction is along x_3.

III. SYMMETRY CONSIDERATIONS

The shape of the precipitate cross section that minimizes the system energy in the absence of an external field may be expected to be one of high symmetry due to the highly symmetric nature of the system. The cross-sectional shape of highest symmetry is a circle and is an energy dictated extremum as predicted by group theory. A first approximation to a cross-sectional shape of a lower symmetry is an ellipse. It is important to recognize that other shapes of lower symmetry, such as squares and rectangles, might possess lower total energies. However, due to the difficulty in treating the elasticity, these lower symmetry forms will not be characterized and we will limit our analyses to elliptical cross sections.

When the precipitate cross section is restricted to be an ellipse, two shape parameters suffice to determine completely the cross section, e.g., the lengths of the semiaxes a and b. Figure 1 shows the model of the precipitate in the matrix and the coordinate system to be used. The semiaxes a and b are taken to lie along the x_1 and x_2 axes, respectively. If any scalar property is plotted as a function of the axes lengths, a and b, an invariance to exchange and orientation of the axes is present. It is advantageous to consider a new set of parameters to maximize the usage of this inherent symmetry. This new coordinate system can be realized by a rotation of axes by 45° in the a-b plane. The new parameters are

$$u = (a - b)/\sqrt{2}\,, \tag{1}$$

$$v = (a + b)/\sqrt{2}\,. \tag{2}$$

The transformation brings a mirror plane into coincidence with the $u = 0$ axis; therefore any scalar property (such as the energy) must be an even function of u. Since we will eventually be searching for energy extremizing shapes at constant cross-sectional area, it becomes convenient to define two new shape parameters. The first parameter is the dimensionless aspect ratio[4]:

$$X = (a - b)/(a + b) \tag{3}$$

and the second parameter is the area of cross section, A. Values of X range from -1 to 1.

Johnson and Cahn[4] show by symmetry that in the absence of an applied stress $X = 0$ is always an energy extremum and that energy extrema other than zero are symmetric about $X = 0$. This symmetry requires that when the total energy is expanded into a power series about $X = 0$ at constant area, the energy must assume the form

$$\Phi(A,X) = \Phi_0(A) + \frac{1}{2!}\Phi_2(A)X^2 + \frac{1}{4!}\Phi_4(A)X^4 + \cdots\,, \tag{4}$$

where Φ_i is the ith derivative of Φ with respect to X at constant A. By differentiating (4) with respect to X and equating to zero, the shapes that extremize the energy can be obtained as a function of the precipitate cross-sectional area and other material parameters. If terms on the order X^5 and higher in the energy expansion are momentarily neglected, the equation of state can be expressed as

$$\left(\frac{\partial\Phi}{\partial X}\right)_A = 0 = X\left(\Phi_2(A) + \frac{1}{3!}\Phi_4(A)X^2\right), \quad (5)$$

the solutions of which are

$$X = 0, \quad X = \pm(-6\Phi_2/\Phi_4)^{1/2}. \quad (6)$$

Depending upon the relative signs of Φ_2 and Φ_4, there may exist a critical cross-sectional area, A_c, at which the circle ($X = 0$) changes stability and other solutions ($X \neq 0$) are possible.

The form of the energy expansion in (4) is the same as that derived by Landau in his theory of second-order phase transitions,[14] where Φ_4 is assumed positive and X is analogous to the "order" parameter (not be confused with the state of coherency of the precipitate–matrix interface); the "disordered" state corresponds to the condition $X = 0 (A < A_c)$ and the "ordered" state corresponds to $X \neq 0 (A > A_c)$. The Landau theory states that at the critical area, A_c, the equilibrium state changes abruptly and the order parameter changes continuously.

If the assumption of $\Phi_4 > 0$ does not hold absolutely, the expansion of $\Phi(A,X)$ must include higher-order terms. It then becomes possible for first-order shape transitions to occur when $\Phi_4 < 0$, i.e., the equilibrium state *and* the order parameter change abruptly. This situation can arise for a very soft precipitate and is discussed later.

The applied stress breaks the symmetry of the system that existed in the absence of the field; $X = 0$ is no longer an energy extremum as predicted by group theory and no longer is the total energy of a precipitate equal for $+X$ and $-X$. If any general scalar property such as the total energy were expanded into a Taylor series about $X = 0$ at constant area for the applied stress case, an expansion of the following form results:

$$\Phi(A,X) = \Phi_0(A) + \Phi_1(A)X + (1/2!)\Phi_2(A)X^2 + (1/3!)\Phi_3(A)X^3 + (1/4!)\Phi_4(A)X^4 + \cdots. \quad (7)$$

Extrema of the energy are determined from solutions to the following equation of state:

$$\left(\frac{\partial\Phi}{\partial X}\right)_A = 0 = \Phi_1(A) + \Phi_2(A)X + (1/2!)\Phi_3(A)X^2 + (1/3!)\Phi_4(A)X^3 + \cdots. \quad (8)$$

Neglecting all terms of X^4 and higher Eq. (8) and assuming that $\Phi_4 > 0$, the equation of state, (8), may have one or three real solutions, none of which are zero. For the case where only one root, X_e, exists, i.e., $D(A) = (8\Phi_2\Phi_4 - 3\Phi_3^2)(\Phi_2^2 - 2\Phi_1\Phi_3) - 2\Phi_1\Phi_2\Phi_3\Phi_4 + 9\Phi_1^2\Phi_4^2 > 0$, it can be shown that $X_e > 0$ for $\Phi_1 < 0$ and $X_e < 0$ for $\Phi_1 > 0$. The transition or sign change of X_e as Φ_1 passes through zero is continuous. When $D(A) < 0$ three solutions exist. The global minimum for this case, X_e, also changes sign as Φ_1 changes sign but does so discontinuously. Therefore we see that the sign of Φ_1 determines the direction in which the energy, and ultimately the shape, is perturbed by the stress.

The coefficient Φ_1 is an implicit function of the applied stress. Changing the applied stress at constant cross-sectional area may induce a change in the sign Φ_1. Thus the following *stress*-induced shape transitions at constant A are also possible:

(1) continuous shape transition if $D(A) > 0$,

(2) first-order shape transition if $D(A) < 0$.

Figure 2 illustrates schematically the behavior of the energy when the cross-sectional area is less than the critical cross-sectional area A_c for various values of Φ_1. So long as $A < A_c$ only one energy extremum is observed. As the sign of Φ_1 (or equivalently the applied stress) passes through zero, the equilibrium shape passes continuously from one distinct shape to another as it passes through zero with no energy barrier. When $A > A_c$, three extrema in the energy may exist as shown in Fig. 3.

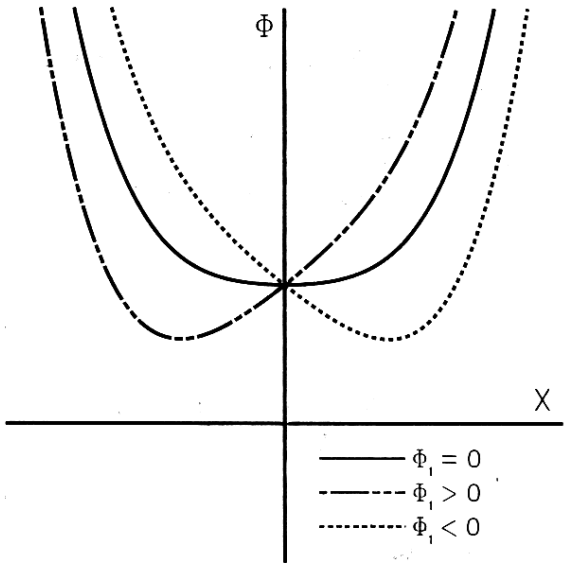

FIG. 2. Stress-induced shape transition for $A < A_c$. The energy Φ is shown schematically as a continuous function of the shape parameter X for various values of Φ_1 at constant cross-sectional area A. The shape parameter changes continuously as Φ_1 changes sign continuously. The transition from one state to another is continuous.

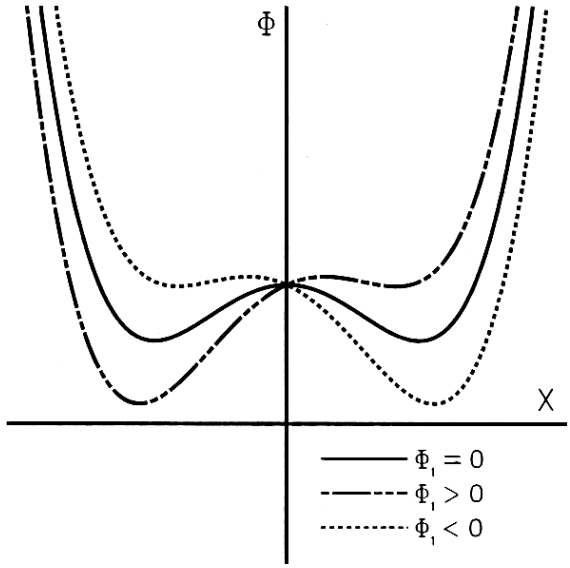

FIG. 3. Stress-induced shape transition for $A > A_c$. The energy Φ is shown schematically as a continuous function of the shape parameter X for various values of Φ_1 at constant cross-sectional area A. The shape parameter (state) changes discontinuously as Φ_1 changes sign continuously. The transition is first-order.

As Φ_1 passes through zero, the equilibrium shape changes discontinuously, the transition in this situation energetically overcoming an energy barrier. Cycling between positive and negative Φ_1 will thus yield a hysterisis in the equilibrium shape. The complete phenomena of size and stress-induced shape transitions can be described in a general way by bifurcation theory (cusp catastrophe[3]).

IV. APPLICATION TO ELASTICALLY INDUCED SHAPE CHANGES

We now examine elastically induced shape transitions within the context of the above analysis. The expressions for the interfacial and elastic strain energy are expressed in terms of X and A to maximize the use of symmetry in the problem. The interfacial energy per unit length can be expressed as

$$E_s = \sigma P , \tag{9}$$

where σ is the interfacial energy density per unit length and P is the circumference of the cross section of the cylinder. The circumference of an ellipse is

$$P = 4\left(\frac{A(1+X)}{\pi(1-X)}\right)^{1/2} E(k), \quad k = \frac{2\sqrt{X}}{(1+X)}, \tag{10}$$

where E is the complete elliptic integral of the second kind and $X \geqslant 0$. The Taylor expansion of the interfacial energy per unit length about $X = 0$ at constant A is[15]

$$E_s = 2\sigma\sqrt{\pi A}\,(1 + \tfrac{3}{4}X^2 + \tfrac{33}{64}X^4 + \tfrac{107}{256}X^6 + \cdots) . \tag{11}$$

The elastic strain energy per unit length elliptic cylinder with elastic constants (μ^*, ν^*), different from the elastic constants of the matrix (μ, ν) and subjected to an applied uniaxial stress, can be derived and expressed as

$$E_w = P_5 + (P_2 X^2 + P_1 X + P_0)/(P_4 X^2 + P_3) , \tag{12}$$

where

$$P_0 = \frac{-4\epsilon^2\mu(1+\delta\kappa)}{(1-2\nu)}\left((1+\omega)^2 + \frac{\delta\omega(1+\omega)q}{(\delta-1)}\right) - \frac{q^2\delta^2\epsilon^2\mu}{2(1-2\nu)}\left(\frac{\kappa(1+\nu)(1-2\nu)(1+\kappa+2\omega)}{(1-\nu)^2} + \frac{2\omega^2(1+\kappa\delta)}{(\delta-1)^2}\right),$$

$$P_1 = \frac{\delta\epsilon^2\mu(1+\nu)(4\nu-\kappa-1)(1+\kappa)}{2(1-\nu)(1-2\nu)}\left(2(1+\omega)q + \frac{\delta\omega q^2}{(\delta-1)}\right),$$

$$P_2 = \frac{4\epsilon^2\kappa\mu[(\delta-1)(1+\omega)^2 + \delta\omega(1+\omega)q]}{(1-2\nu)} + \frac{\delta^2\epsilon^2\mu q^2}{2(1-2\nu)}\left(\frac{(1+\nu)^2(1-2\nu)(1+\kappa+2\kappa\omega)}{(1-\nu)^2} + \frac{2\kappa\omega^2}{(\delta-1)}\right),$$

$$P_3 = (1+\delta\kappa)(2\omega+\kappa+1) ,$$

$$P_4 = -(\delta-1)(2\kappa\omega+\kappa+1) ,$$

$$P_5 = \frac{2\epsilon^2\mu(1+\omega)}{(1-2\nu)}\left(1 + \frac{\delta q}{(\delta-1)}\right) + \frac{\delta^2\epsilon^2\mu q^2}{2(\delta-1)}\left[\left(\frac{1+\nu}{1-\nu}\right)^2 + \frac{\omega}{(\delta-1)(1-2\nu)}\right],$$

and where

$$\omega = [(\delta-1) + 2\delta\nu\psi_0], \quad \psi_0 = \frac{(1-2\nu)(\nu^*)}{(1-2\nu^*)(\nu)} - 1 ,$$

$$\delta = \frac{\mu^*}{\mu}, \quad \tau = \frac{T}{E}, \quad \kappa = 3 - 4\nu ,$$

$$q = \frac{(1-\nu)(1-\delta)}{\epsilon\delta} , \tag{13}$$

Here E is Young's modulus and T is the applied stress assumed to be directed along the x_2 (b) axis. Note that $\psi_0 = 0$ and $\omega = (\delta - 1)$ when $\nu = \nu^*$.

Following earlier work,[4] the total energy and precipitate size can be expressed in dimensionless form. The dimensionless energy Φ and dimensionless size λ are defined as

$$\Phi = (E_s + E_w)/2\sigma\sqrt{\pi A} , \tag{14}$$

$$\lambda = (A/A_c)^{1/2} . \tag{15}$$

The critical area A_c is the cross-sectional area at which

the circle becomes unstable in the absence of the applied stress. It is determined by the intersection of the two solutions to the equation of state in Eq. (6), i.e., when

$$\left(\frac{\partial\Phi^2}{\partial X^2}\right)_{X=0} = 0 \quad (\tau = 0) . \tag{16}$$

Solving for the critical area gives

$$\sqrt{A_c} = \frac{3\sqrt{\pi}\sigma(\delta\kappa+1)(1-2\nu)(2\omega+\kappa+1)^2}{8\epsilon^2\mu(1-\delta)(\kappa^2-1)(1+\omega)^2} . \tag{17}$$

Here A_c is physically meaningful only for precipitates elastically softer than the matrix, $\delta < 1$. Elastically hard precipitates do not experience a bifurcation and circular cylinders are always the stable shape in the absence of an applied stress. Consequently, unless otherwise indicated, our analysis will be restricted to elastically soft precipitates.

The dimensionless energy Φ can be expanded in a Taylor series about $X = 0$ where $\nu = \nu^*$ and $|q| \ll 1$. The expansion assumes the following relatively simple form for terms up to X^6:

$$\begin{aligned}
\Phi = &\left[1 - \frac{3(1+\delta\kappa)[2(\delta-1)+(1+\kappa)]}{8\delta(\delta-1)(\kappa-1)}\left(\frac{\kappa-1}{\kappa+1}+\frac{\delta q}{(\delta-1)}\right)\lambda\right] \\
&+\left(\frac{3(1+\nu)[2(\delta-1)+(1+\kappa)](1+\kappa-4\nu)q}{16(\delta-1)(\kappa-1)(1-\nu)}\lambda\right)X + \frac{3}{4}[1-(1+q)\lambda]X^2 \\
&+\left(\frac{3(1+\nu)[2(1+\delta\kappa)-(1+\kappa)](1+\kappa-4\nu)q}{16(1+\delta\kappa)(\kappa-1)(1-\nu)}\lambda\right)X^3 \\
&+\frac{33}{64}\left(1-\frac{64(\delta-1)[2(1+\delta\kappa)-(1+\kappa)](1+q)}{11(1+\delta\kappa)[2(\delta-1)+(1+\kappa)]}\lambda\right)X^4 \\
&+\left[\frac{3(\delta-1)(1+\nu)[2(1+\delta\kappa)-(1+\kappa)]^2(1+\kappa-4\nu)q}{16(1+\delta\kappa)^2(\kappa-1)(1-\nu)[2(\delta-1)+(1+\kappa)]}\lambda\right]X^5 \\
&+\frac{107}{256}\left(1-\frac{192(\delta-1)^2[2(1+\delta\kappa)-(1+\kappa)]^2(1+q)}{107(1+\delta\kappa)^2[2(\delta-1)+(1+\kappa)]^2}\lambda\right)X^6 .
\end{aligned} \tag{18}$$

Note that $\lambda = 1$ defines the bifurcation point in the absence of an applied stress and that the fourth-order term is not always positive, thus the inclusion of higher-order terms.

The energy extrema are determined by differentiating Φ with respect to X at constant A and equating to zero:

$$\begin{aligned}
\frac{\partial\Phi}{\partial X} = 0 = &\left[\frac{3(1+\nu)[2(\delta-1)+(1+\kappa)](1+\kappa-4\nu)q}{16(\delta-1)(\kappa-1)(1-\nu)}\lambda\right] + \frac{3}{2}[1-(1+q)\lambda]X \\
&+\left(\frac{9(1+\nu)[2(1+\delta\kappa)-(1+\kappa)](1+\kappa-4\nu)q}{16(1+\delta\kappa)(\kappa-1)(1-\nu)}\lambda\right)X^2 \\
&+\frac{33}{16}\left(1-\frac{64(\delta-1)[2(1+\delta\kappa)-(1+\kappa)](1+q)}{11(1+\delta\kappa)[2(\delta-1)+(1+\kappa)]}\lambda\right)X^3 \\
&+\left(\frac{15(\delta-1)(1+\nu)[2(1+\delta\kappa)-(1+\kappa)]^2(1+\kappa-4\nu)q}{16(1+\delta\kappa)^2(\kappa-1)(1-\nu)[2(\delta-1)+(1+\kappa)]}\lambda\right)X^4 \\
&+\frac{321}{128}\left\{1-\frac{192(\delta-1)^2[2(1+\delta\kappa)-(1+\kappa)]^2(1+q)}{107(1+\delta\kappa)^2[2(\delta-1)+(1+\kappa)]^2}\lambda\right\}X^5 .
\end{aligned} \tag{19}$$

The extremizing values of X can then be obtained as a function of λ and q. The loci of points for each solution defines a bifurcation branch that is continuous in λ.

V. DISCUSSION

A. Shape transitions and stability

In the presence of the applied stress and for small values of λ, only one extremizing shape exists, X_e. When $\Phi_1 < 0$, $X_e > 0$, while when $\Phi_1 > 0$, $X_e < 0$. The sign of Φ_1 is determined by the parameter q defined by Eq. (13). For elastically soft precipitates, the sign of q is fixed by the sign of τ/ϵ.

The sign of Φ_4 determines the order of the size-induced shape transition in the absence of an applied stress for an elastically soft precipitate. When $\Phi_4 > 0$,

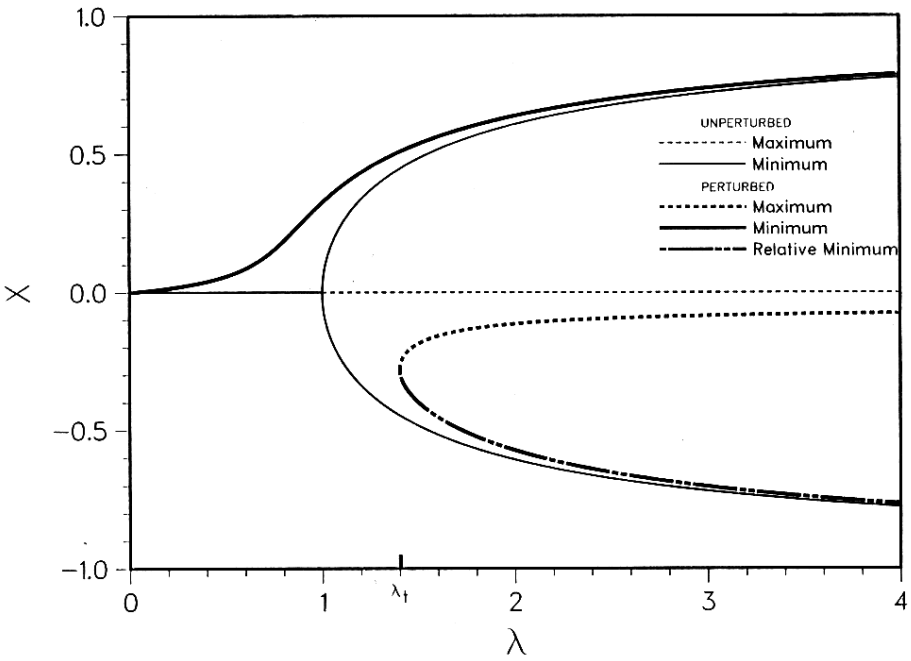

FIG. 4. Bifurcation diagram of energy extremizing shapes as a function of the nondimensional size, λ, for $\Phi_4 > 0$, $\delta = 0.8$, and $\nu = \nu^* = \frac{1}{3}$. Thin lines represent the unperturbed bifurcation $q = 0$. Heavy lines represent the perturbed bifurcation $q = 0.01$. The second-order size-induced shape transition for $q = 0$ occuring at $\lambda = 1$ is absent for $q \neq 0$.

the size-induced shape transition is second order and occurs when $\Phi_2 = 0$. The size-induced shape transition is first order when $\Phi_4 < 0$. As will be shown, this condition can be realized in Eq. (13) for precipitates much softer than the matrix.

Figures 4 and 5 compare the energy extremizing solutions for the perturbed and unperturbed bifurcations when $\Phi_4 > 0$. In both figures heavy lines denote the perturbed bifurcation ($q \neq 0$) and thin lines denote the unperturbed bifurcation ($q = 0$). The material constants employed are $\delta = 0.8$ and $\nu = \nu^* = \frac{1}{3}$. Once the cylinder reaches a critical cross-sectional area for the unperturbed situation ($\lambda = 1$), the equilibrium state changes sharply, and the shape continuously, from a circular to an elliptical cylinder with no particular spatial orientation. No metastable states exist. Under the influence of an applied stress directed along the b axis of the precipitate and assuming the misfit and applied stress are of the same sign ($q > 0$), the equilibrium shape is that of an elliptical cylinder whose major axis is perpendicular to the stress axis, as shown in Fig. 4. When the misfit and stress are of opposite sign ($q < 0$), the

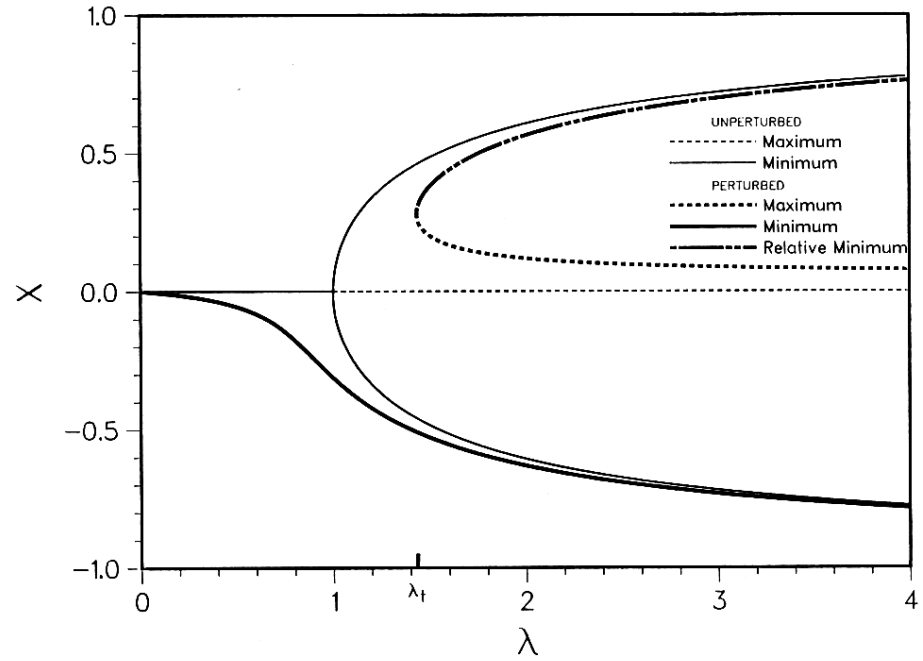

FIG. 5. Bifurcation diagram of energy extremizing shapes as a function of the nondimensional size, λ, for $\Phi_4 > 0, \delta = 0.8$, and $\nu = \nu^* = \frac{1}{3}$. Thin lines represent the unperturbed bifurcation $q = 0$. Heavy lines represent the perturbed bifurcation $q = -0.01$. The second-order size-induced shape transition for $q = 0$ occurring at $\lambda = 1$ is absent for $q \neq 0$.

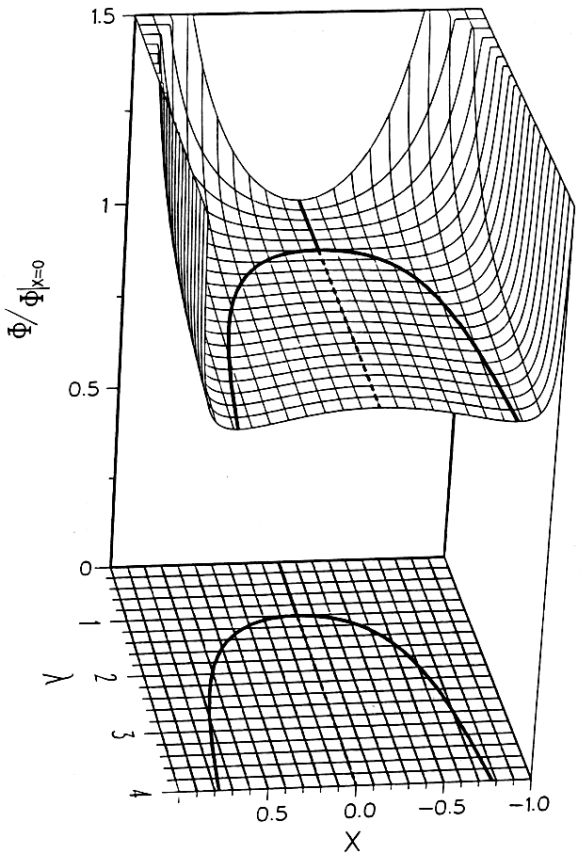

FIG. 6. Total energy, $\Phi(\lambda,X)/\Phi(\lambda,0)$, as a function of size, λ, and shape, X, for $\Phi_4>0$, $\delta=0.8$, $\nu=\nu^*=\frac{1}{3}$, and $q=0$. Energy extrema are superimposed on the surface and projected onto the λ-X plane. Solid lines represent minima, dashed lines maxima.

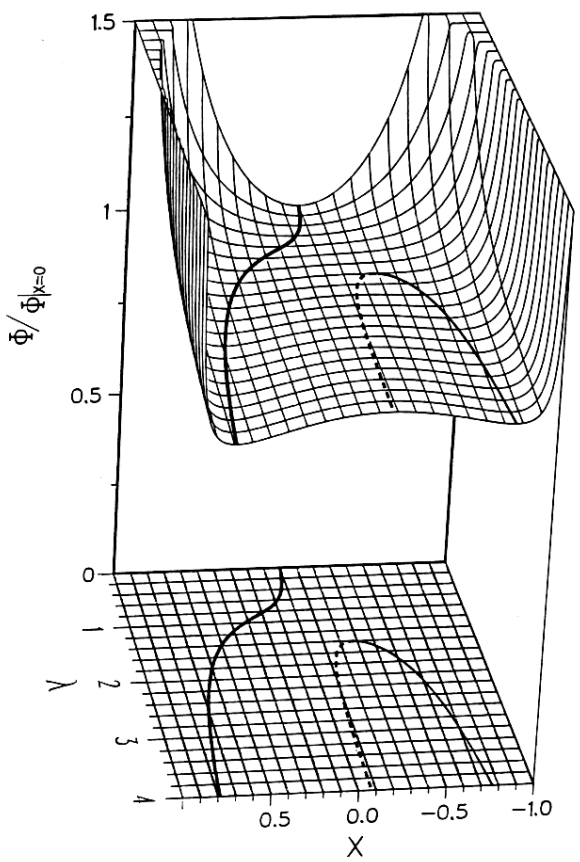

FIG. 7. Total energy, $\Phi(\lambda,X)/\Phi(\lambda,0)$ as a function of size, λ, and shape, X, for $\Phi_4>0$, $\delta=0.8$, $\nu=\nu^*=\frac{1}{3}$, and $q=0.01$. Energy extrema are superimposed on the surface and projected onto the λ-X plane. Solid lines represent minima, dashed lines maxima, and chain-dashed lines metastable extrema.

shape is that of an elliptical cylinder whose major axis is aligned parallel to the stress axis, as shown in Fig. 5. For values of $\lambda>2$, Figs. 4 and 5 show that the stable and metastable precipitate shapes for the perturbed case are very close to that of the unperturbed stable shapes. Thus it can be concluded that unloading the system for $\lambda>2$ results in only a small change in the precipitate shape. The elastically soft precipitate shape is affected most for $\lambda<2$, changing from a circular to an elliptic cross section for $\lambda\leqslant 1$.

The relationship between the shape, size, and energy is displayed in Figs. 6 and 7, where Φ is plotted as a function of λ and X for the conditions stated in Fig. 4. Figure 6 depicts the case when $q=0$ and Fig. 7 where $q=0.01$. A trace of the energy extrema is superimposed onto the energy surface and then projected onto the λ-X plane to reproduce Figs. 3 and 4, respectively. Although Fig. 4 shows that the stable and metastable precipitate shapes for $q\neq 0$ approach the stable shapes for $q=0$, Fig. 7 shows that the energy difference between the stable and metastable precipitate shapes becomes larger as λ increases. Thus the stability of the stable shape becomes more pronounced as λ increases and also as q increases.

Figures 4–7 illustrate the effect of an applied stress on the energy extremizing shape for the case where $\Phi_4>0$. When $q=0$, $X=0$ is a minimum energy condition when $\lambda\leqslant 1$, and an energy maximum when $\lambda>1$. In addition to the energy maximum when $\lambda>1$, there exist two congruent minima, $X\neq 0$, which are symmetric about the λ axis. When $q\neq 0$ the situation changes. The energy minimum is defined by the same solution to the

equation of state for all λ, therefore there is no longer a size-induced shape transition. Two additional extrema appear at a turning point λ_t, one extrema is a relative minimum the other is an energy minimum. The value of λ at which the turning point occurs depends on the magnitude of the applied stress and the material parameters.

Figure 8 depicts a bifurcation diagram for the case in which $\Phi_4 < 0$ and $q = 0$. This occurs when the precipitate is much softer than the matrix. The materials constants used in calculating Fig. 8 are $\delta = 0.01$ and $\nu = \nu^* = \frac{1}{3}$. The circular cylinder is stable for $\lambda < \lambda_c$ with two metastable states present for $\lambda_t \leqslant \lambda \leqslant \lambda_c$, where λ_c is defined as the precipitate size where the two states, $X = 0$ and $X = \pm X_c$, are in equilibrium. Beyond λ_c the circular cylinder becomes metastable with respect to the elliptical cylinder, the equilibrium size-induced transition occuring discontinuously. The circular cylinder remains metastable up to the bifurcation point, $\lambda = 1$, becoming unstable beyond $\lambda = 1$. The first-order size-induced shape transition shown in Fig. 8 is from $X = 0$ to $X_c = 0.906$ at $\lambda_c = 0.803$. The turning point in Fig. 8 is located at $X_t = 0.838$ and $\lambda_t = 0.757$. A first-order transition is shown to be possible by the Taylor expansion although the conditions for the transition are overestimated. Because the elliptic integral of the second kind used to calculate the interfacial energy converges much more slowly than the elastic strain energy, the Taylor series expanded to sixth order in Eq. (18) is valid only for X close to zero. Using Eq. (18), the condition needed for a first-order transition, $\Phi_4 < 0$, is realized for $\delta < 0.132$ when $\nu = \nu^* = \frac{1}{3}$. Solving Φ numerically using Eq. (14), a first-order transition is observed approximately an order of magnitude less than $\delta \approx 0.132$ when $\nu = \nu^* = \frac{1}{3}$.

The effect of an applied stress on the shape of an elastically hard precipitate also depends on the sign of q and exhibits only one extrema in energy regardless of the precipitate size. As expected from group theory, the precipitate cross-sectional shape is no longer circular in the presence of an applied stress. The cross-sectional shape is always elliptical and the shape change due to the applied stress becomes greater as the precipitate size increases. For $q > 0$, the major axis of the precipitate aligns perpendicular to the stress axis. The major axis aligns parallel to the stress axis when $q < 0$.

The type of possible transitions can also be enumerated. As noted in Figs. 4 and 5, the situation of $q = 0$ shows a second-order size-induced shape transition at $\lambda = 1$ for an elastically soft precipitate. There is no size-induced shape transition in the λ-X plane for $q \neq 0$. However, there exists both a first-order and continuous stress-induced shape transition if we were to examine the X-q plane. The continuous stress-induced transition occurs for $\lambda \leqslant 1 (A \leqslant A_c)$, X changing continuously from one state to another as q goes through zero. A first-order transition (or hysterisis) in the λ-q plane exists for $\lambda > 1 (A > A_c)$ as X changes discontinuously as q passes through zero. This is exhibited in Fig. 9. The stress-induced shape transition for an elastically hard precipitate is continuous regardless of the size of the precipitate.

Upon examination of Figs. 4 and 5, the effects of stress on the precipitate shape relative to the unstressed case can be discussed. There is a distinct change in the

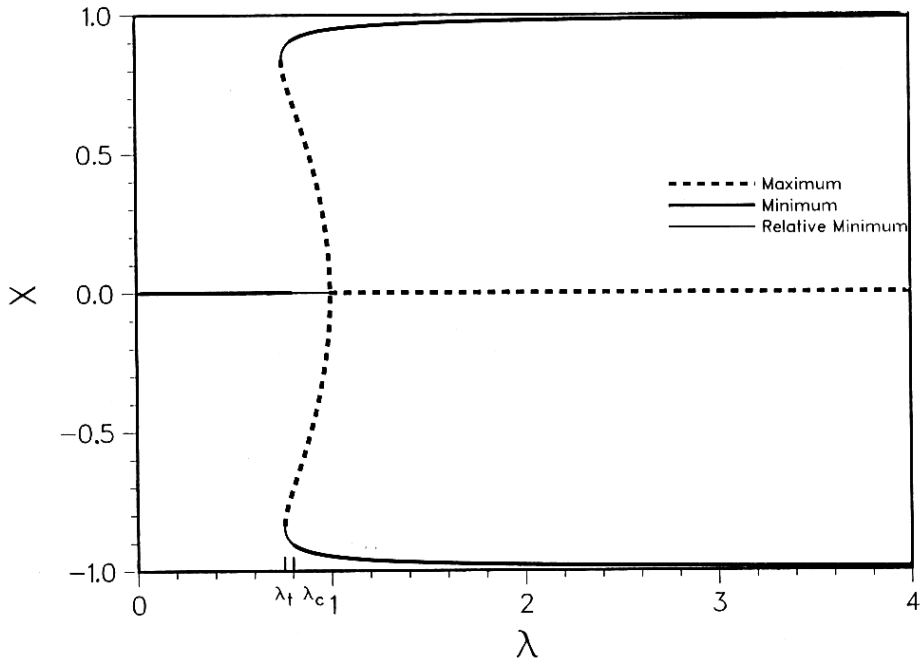

FIG. 8. Bifurcation diagram of energy extrema for $\Phi_4 < 0$, $\delta = 0.01$, $\nu = \nu^* = \frac{1}{3}$, and $q = 0$. A first-order size-induced shape transition occurs at the critical point ($\lambda_c = 0.803$), the equilibrium shape making a pronounced discontinuous jump from a circular ($X = 0$) to an elliptical cylinder ($X_c = \pm 0.906$).

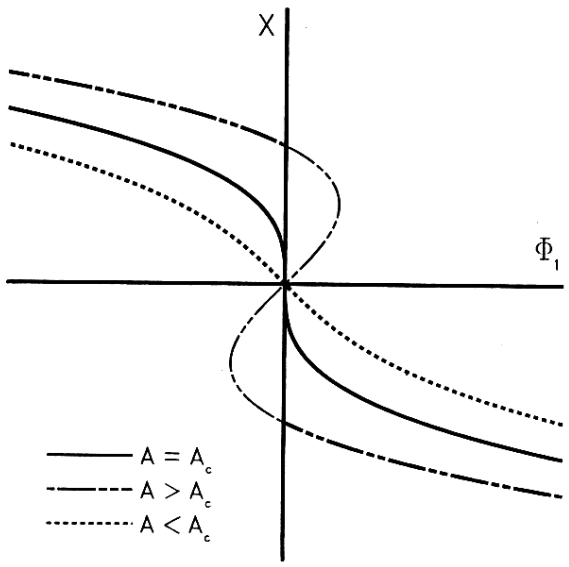

FIG. 9. Energy extrema are shown as a function of the perturbation parameter, Φ_1, for various values of the cross-sectional area A. Heavy lines represent stable solutions and light lines represent metastable or unstable solutions. For $A \leqslant A_c$, X changes continuously with Φ_1, the transition from $+X$ to $-X$ representing a continuous stress-induced shape transition. For $A > A_c$, X changes discontinuously with q as q passes through zero. This transition is first order.

equilibrium precipitate shape for $\lambda \leqslant 1$. The circular cylinder becomes an elliptic cylinder regardless of the magnitude of the stress. When $\lambda \gg 1$ there is relatively little change in precipitate shape, the shape parameter X approaching the unstressed condition asymptotically. For an elastically hard precipitate, the shape difference between the unstressed and stressed cases becomes greater as the precipitate size increases.

Falk discussed similar stress effects using a Taylor expansion in describing martensitic phase transformations.[16] He concludes that there is no stress-induced phase transition from one equilibrium state to another if a constant external stress is applied to the system (i.e., the initial disordered state remains stable), yet shows a hysteresis in the order parameter in the ordered region ($A < A_c$) as the sign of the stress is changed, all other conditions held constant. Falk also determined that the change in the order parameter for the stressed condition is significantly different from the order parameter in the unstressed condition only for the disordered region ($A < A_c$) and the intermediate vicinity of the critical point ($A \geqslant A_c$). For conditions beyond the critical point, the value of the order parameter in the stressed state asymptotically approaches that of the unstressed state.

The symmetry predictions of group theory are supported by the energy results shown in Figs. 4 and 5. For the unstressed system, group theory predicts that the circular cross section of an elastically soft or hard precipitate is an energy extremum and that the extremum could be stable, unstable, or a saddle. In retrospect, we see that the circular cross section is stable for $\lambda \leqslant 1$ and unstable for $\lambda > 1$ for the case of elastically soft precipitates and stable for all λ for the case of elastically hard precipitates. By applying a uniaxial stress to a system, group theory predicts that the circular cylinder is no longer an energy extremum but a precipitate with the symmetry of an elliptical cross section is. This is exactly the result found. An estimate of the size at which a shape transition occurs can be simply determined from knowledge of the specific material parameters of a system. As an example, we choose the shear modulus of the matrix to be 5×10^{10} J/m^3 and Poisson's ratio for both matrix and precipitate to be $\frac{1}{3}$. The interfacial energy of the coherent precipitate in the matrix is assumed to be 3 J/m^2. If the precipitate is elastically softer than the matrix, $\delta = 0.8$, and the misfit is $\epsilon = 0.001$, then the critical area is $A_c = 4.9 \times 10^{-7}$ m^2. If the misfit is increased to 0.01 then the critical area is $A_c = 4.9 \times 10^{-11}$ m^2.

B. Precipitate orientation

Changes in the variant morphology, or the orientations a precipitate can attain, are changes in symmetry. (Here, variant morphology is defined as the physical collection or mathematical ensemble of all the possible spatial orientations a precipitate of a given shape can possess under equilibrium conditions.) The minimum *symmetry* of the equilibrated variant morphology in the absence or presence of an external influence is determined by intersecting the point group symmetries of the precipitate and the matrix with the limiting group symmetry of the external field, accounting for the orientational relationship between them.[11,13,17–21] This convention of symmetry intersection or superposition is called the *Curie principle*. The Curie principle is a generalization of the Neumann principle.[17,21,22] However, because there can be many representations of variant morphologies that exhibit a particular symmetry, the equilibrium variant morphology cannot be determined exactly by group theory treatments. The actual variant morphologies must be determined by using the analytical expressions for the elastic strain and interfacial energies. The usefulness of using group theory to predict variant morphology symmetries rests on its ability to indicate orientation extrema, thus providing a *limited* set of energy calculations that need to be made.

In the absence of an applied stress, the spatial orientation of the ellipse axes are all equivalent and an infinite number of equally possible orientations exist. This situation is easily realized from group theory principles. If the symmetry elements of the precipitate and the matrix are superimposed in the same frame of reference, the intersection group contains at least the symmetry elements of the variant morphology present. For the case

of an elastically isotropic elliptical cylinder in an elastically isotropic matrix

$$\begin{array}{cccc} \mathbf{G_p} & & \mathbf{G_m} & \mathbf{G_{vm}} \\ \infty/\infty m & \cap & \infty/\infty m & = \infty/\infty m \\ & & & \downarrow \\ & & & \infty m \text{ (in two dimensions)} \end{array}, \quad (20)$$

where $\mathbf{G_p}$ represents the group of symmetry elements for the precipitate point group, $\mathbf{G_m}$ represents the group of symmetry elements for the matrix point group, and $\mathbf{G_{vm}}$ represents the group of symmetry elements for the variant morphology. Equation (20) also makes use of the limiting point symmetry groups where ∞ represents an infinite rotation axis, / implies a rotation axis that is not necessarily orthogonal to the primary rotation axis, and, specifically for the two-dimensionally cross section, the ∞ implies an infinite rotation axis normal to the cross section and m implies an arbitrary mirror containing that ∞ axis. This means that the system *must* have an infinite number of possible orientations in the absence of an applied stress. Whether the cross section of the precipitate is circular or elliptical is indeterminable, but the distribution of possible orientations a precipitate of a given shape can have includes an infinite number of possible orientations of the same probability with respect to a fixed reference frame. Therefore it is unnecessary to perform an orientation-dependent energy calculation.

In the presence of an external field, the symmetry of the variant morphology is broken. By superimposing the symmetry elements of the applied stress with the unstressed distribution symmetry, the minimum symmetry of the final variant morphology results. The morphology could have more symmetry, but not less than that resulting from the superposition.[13,17] For the case of a uniaxial stress applied perpendicular to the infinite axis this can be expressed as

$$\begin{array}{cccccc} \mathbf{G_p} & & \mathbf{G_m} & & \mathbf{G_i} & \\ \infty/\infty m & \cap & \infty/\infty m & \cap \frac{\infty}{m} mm = \frac{\infty}{m} mm & \subseteq & \mathbf{G_{vm}} \\ & & & \downarrow & & \cup \\ & & \text{(in two dimensions)} & 2mm & & 2mm \end{array}, \quad (21)$$

where $\mathbf{G_i}$ represents the group of symmetry elements of the external influence. If we consider the example of $\mathbf{G_B} \supseteq \mathbf{G_A}$, the symbol $\supseteq$ means that the symmetry of **B** is equal to or greater than the symmetry of **A**, or equivalently, **A** is a subgroup of **B**.

For the condition of equality in (21), the symmetry requires one of three variant morphologies or orientation distributions:

(1) a precipitate aligned with the major axis of the cross section parallel to the stress axis ($2mm$ symmetry),

(2) a precipitate aligned with the major axis of the cross section perpendicular to the stress axis ($2mm$ symmetry),

(3) A precipitate aligned with the major axis of the cross section at an angle $\pm\theta$ to the stress axis, where $\theta \neq 0$, $\pi/4$, or $\pi/2$ ($2mm$ symmetry).

Which one of the variations or combinations of the variations listed above is actually present depends strictly on system parameters. Because symmetry rules can only predict conditions qualitatively, exact energy expressions must be developed as a function of shape, orientation, and system material parameters to differentiate energy minima from maxima. Cases 1 and 2 are those examined above by exact energy calculations.

Effects of an influence on a medium can also result in *higher* symmetry than the minimum symmetry predicted by the intersection of the point groups of the influence and the medium.[13,17] Usually, special conditions give rise to higher symmetry. For example, tungsten is a cubic material yet it exhibits isotropic elasticity because of a relationship between the elastic compliance coefficients ($S_{11} - S_{12} = 2S_{44}$). The symmetry of the variant morphology can also result in cross sections with higher symmetry than $2mm$. Possible symmetries would be $4mm$, $6mm$, ..., or ∞mm.

The potential usefulness of analyses of this nature for alloy design can be realized for many situations. Multi-phase materials might be processed to exhibit only desired orientations (variants) to control mechanical or physical properties.[8] In other words, knowledge of the stability of the orientations (variants) of the precipitates in an external field could be used to select the field necessary to produce a desired morphology. Another application focuses on alloy selection of a material to be used in an external field where a stable morphology is required. A material could be selected to exhibit a particular precipitate shape or variant morphology in an external field based on the proper choice of system material parameters. In applications where stress is cycled between tensile and compressive modes and stable shapes are required, the order of the transition in orientation due to stress becomes important. First-order transitions far removed from conditions dictating higher-order transitions are advantageous due to kinetic considerations; a large activation energy may have to be overcome for the precipitate to change shape.

VI. CONCLUSIONS

This work has examined a generic technique for determining equilibrium precipitate morphologies and shape transitions in the presence of an applied stress.

Specific calculations were performed for an isolated elliptical cylinder in an infinite matrix under the influence of a uniaxial stress and the nature of the shape transitions determined as a function of precipitate size, coherency strains, elastic coefficients, and interfacial energy density for isotropic systems. The analysis was based on two parts: qualitative predictions based on symmetry rules and exact solutions based on elasticity calculations. Aspects of bifurcation theory were used to illustrate the problem in a general way and to compare the transitions with other known transitions. The details of the energy expressions showed that bifurcations or shape transitions in the absence of an applied stress occur only when the precipitate is elastically softer than the matrix, and do so from only one bifurcation point; there are no bifurcations off of bifurcations. A uniaxial stress breaks the unperturbed bifurcation results. There is no longer a size-induced shape transition from one bifurcation branch to another, as observed for elastically soft precipitates.

The order of the size-induced shape transition in the absence of an applied stress is governed by the sign of the fourth derivative of the total energy with respect to the shape parameter, Φ_4. For an elastically soft precipitate, the transition is second-order if $\Phi_4 > 0$ and is first-order if $\Phi_4 < 0$.

The sign of the first derivative of the energy with respect to the shape parameter, Φ_1, determines the direction the energy or equilibrium shape is perturbed by an applied stress. When $\Phi_1 > 0$, the major axis aligns with the stress axis ($X_e < 0$), and aligns perpendicular to the stress axis when $\Phi_1 < 0$ ($X_e > 0$). Here Φ_1 is proportional to $-\tau(1-\delta)/\epsilon$ or $-q$.

Stress-induced shape transitions are also observed. The transition is continuous for $\lambda \leqslant 1$ and first-order for $\lambda > 1$ when the precipitate is elastically softer than the matrix ($\delta < 1$), and continuous for all λ when the precipitate is elastically harder than the matrix ($\delta > 1$).

Group theory can be implemented to qualitatively predict the orientation the precipitate will take in the presence of an applied stress. These orientations are not definite, however.

ACKNOWLEDGMENTS

We wish to acknowledge the support of the Division of Materials Science of the Department of Energy under grant DE-FG02-84ER45166.

REFERENCES

[1]A. J. Ardell and R. B. Nicholson, Acta Metall. **14**, 1295 (1966).
[2]G. Iooss and D. D. Joseph, *Elementary Stability and Bifurcation Theory* (Springer, Berlin, 1980).
[3]T. Poston and I. Stewart, *Catastrophe Theory and its Applications* (Pitman, Boston, 1978).
[4]W. C. Johnson and J. W. Cahn, Acta Metall. **32**, 1925 (1984).
[5]J. K. Tien and S. M. Copley, Metall. Trans. **2**, 215 (1971).
[6]T. Miyazaki, K. Nakamura, and H. Mori, J. Mater. Sci. **14**, 1827 (1979).
[7]T. Eto, A. Sato, and T. Mori, Acta Metall. **24**, 559 (1976).
[8]R. A. MacKay and L. J. Ebert, Metall. Trans. A **16**, 1969 (1985).
[9]P. Kournettes and K. Stierstadt, Philos. Mag. B **51**, 381 (1985).
[10]J. C. Bacri and D. Salin, J. Phys. (Paris) Lett. **43**, L649 (1982).
[11]J. W. Cahn and G. Kalonji, *Solid→Solid Phase Transformations*, edited by H. I. Aaronson, D. E. Laughlin, R. F. Sekerka and C. M. Wayman (T. M. S.-A. I. M. E., Warrendale, PA, 1982), pp. 3–14.
[12]M. Guymont, Phys. Rev. B **24**, 2647 (1981).
[13]Y. I. Sirotin and M. P. Shaskolskaya, *Fundamentals of Crystal Physics* (Mir, Moscow, 1982), p. 429
[14]L. D. Landau and E. M. Lifshitz, *Statistical Physics* (Pergamon, Oxford, 1980), 3rd ed., Chap. XIV.
[15]P. F. Byrd and M. D. Friedman, *Handbook of Elliptic Integrals for Engineers and Scientists* (Springer, New York, 1971).
[16]F. Falk, J. Phys. (Paris) Colloq. **43**, C4-3 (1982).
[17]V. A. Koptsik, Sov. Phys. Crystallogr. **2**, 95 (1957).
[18]I. S. Zheludev, Sov. Phys. Crystallogr. **2**, 330 (1957).
[19]P. Curie, J. Phys. (Paris) **3**, 393 (1894).
[20]N. V. Perelomova and M. M. Tagieva, *Problems in Crystal Physics with Solutions* (Mir, Moscow, 1983), Chap. 2.
[21]J. Kocinski, *Theory of Symmetry Changes at Continuous Phase Transitions* (Elsevier, New York, 1983), pp. 162–172.
[22]J. F. Nye, *Physical Properties of Crystals* (Clarendon, Oxford, 1979), pp. 20–24.